International Journal of Control, Energy and Electrical Engineering (CEEE)
Vol.9 pp.1-5

Structural, dielectric and piezoelectric properties of (1-x) Pb ($Zr_{0.52}$ $Ti_{0.48}$) O_3–x Sm Cr O_3 ceramics

F. Kahoul[*1,2], L. Hamzioui[1,2], A. Guemache[1], M.Aillerie[3,4], A. Boutarfaia[2]

[1]*Université de M'Sila, Département Socle Commun ST, Faculté de Technologie, M'Sila 28000 Algérie*

[2]*Université de Biskra, Département de Chimie, Laboratoire de Chimie Appliquée, B. P. 145, RB-Biskra 07000 Algérie*

[3]*Université de Lorraine, LMOPS, EA 4423, 57070 Metz, France*

[4]*Centrale Supelec, LMOPS, 57070 Metz, France*

fares.kahoul@univ-msila.dz

***Abstract*— This work reported the structural, dielectric, and piezoelectric behavior of (1-x) Pb ($Zr_{0.52}$ $Ti_{0.48}$) O_3 – x Sm Cr O_3 ceramics (abbreviated as PZTSC, where x = 0.005, 0.01, 0.015, 0.02 and 0.025), were prepared by the traditional solid-state reaction method. The phase transition, microstructure, dielectric, piezoelectric properties, and the temperature stability of the ceramics were investigated. X-ray diffraction analysis indicated that as-prepared ceramics were of pure perovskite phase and the possible morphotropic phase boundary (MPB) between the tetragonal and rhombohedral phase compositions were located near the SC content of x ≥ 0.02, confirmed by their corresponding dielectric and piezoelectric properties. All specimens present high relative density above 97%, indicating a wide sintering window for this system. Microstructural investigations of all the samples reveal that SC doping inhibits grain growth. The dielectric and piezoelectric properties show a maximum response at x ≥ 0.02, which corresponds to the morphotropic phase boundary (MPB).**

***Keywords*— XRD, Dielectric Properties, Piezoelectric Properties, MPB, Density**

I. INTRODUCTION

The high power characteristics of piezoelectric materials have been investigated for device applications in ultrasonic motors, piezoelectric actuators, piezoelectric transformers, ultrasonic vibrator, filter, blue luminescence and resonator, and medical applications [1–5].

For high-power multilayer piezoelectric device applications, piezoelectric materials are electrically driven to high mechanical vibration near the resonance frequencies, leading to a temperature rising and deterioration of piezoelectric properties with the increase of their vibration velocities [6,7]. Therefore, the lead-based piezoelectric ceramics should have high piezoelectric constant (d_{31}), high electromechanical coupling factor (k_p), high mechanical quality factor (Q_m), and good temperature stability [8,9].

The $Pb(Zr_xTi_{1-x})O_3$ system and its modified solid solutions are known to exhibit excellent dielectric and elastic properties at the "Morphotropic Phase Boundary (MPB)" [10–13]. This MPB is believed to be a coexistence region of two phases namely, tetragonal and rhombohedral phases and still is a topic of great debate [14–22].

In general, PZT system ceramics should be sintered at high temperatures between1100 and 1300 °C in order to obtain complete densification. Accordingly, environmental pollution due to its PbO evaporation and the use of expansive Pd rich Ag/Pd internal electrode in case of manufacturing multilayer ceramic actuator are inevitable.

Hence, to reduce its sintering temperature, various kinds of material processing methods such as hot pressing, high energy mill, liquid phase sintering, and using ultra fine powder have been performed. Among these methods, liquid phase sintering is basically an effective method for aiding densification at low temperature. The theoretical explanation for liquid phase sintering was already reported over 40 years ago.

In this work, the phase structure, density, electrical properties, low-temperature sintering and temperature characteristics of PZTSC piezoelectric ceramics were described systemically. The aim of the work was to find out the optimized content of Sm_2O_5 and Cr_2O_3, which can make this system have higher electrical properties for multilayer piezoelectric device applications.

II. EXPERIMENTAL PROCEDURE

PZTSC ceramics having the chemical formula of (1-x) Pb ($Zr_{0.52}$ $Ti_{0.48}$) O_3 – x Sm Cr O_3, where x = 0.005, 0.01, 0.015, 0.02 and 0.025), were prepared by the mixed oxide route.

An appropriate mixture of pure oxides (purities >99 %) were ball milled for 24 h using ZrO_2 media with distilled water. The mixture was then dried and calcined at 850 °C for 3h. The calcined powder was again ball milled to achieve1.2 µm particle size. This was followed by mixing of 10 wt.% of PVA as a binder in the calcined powder and the specimens were pressed using uniaxial press. Specimens were subsequently sintered in a PbO rich atmosphere between 1150 °C for 2 h and final dimension obtained after lapping was12 mm diameter and 1mm thickness.

The density of the sintered samples was measured using Archimedes' principle. Microstructural features such as a grain size and pores were characterized by means of atomic force microscopy (AFM). The sintered pellets were electroded with high-purity silver paste and fired at 700 °C for 1 h. The samples were pooled in a silicon oil bath at 120 °C for 1 h under a static DC electrical field of 4.5 kV/mm.

ISSN 2356-5608

Powder X-ray diffraction (XRD) measurements were carried out using a Rigaku X-ray diffractometer with Cu K_α. The XRD patterns were recorded at a scan rate of 2°/min for 2θ varying from 10º to 80°. Temperature-dependent dielectric constant (ε_r) and tangent loss (tanδ) were obtained as the functions of temperature using a inductance capacitance resistance meter (LCR, HIOKI, Model-3532-50) in a proportional integral derivative (PID) controlled heating chamber.

Twenty four hours after poling, the piezoelectric properties: piezoelectric constant (d_{31}), electromechanical planar coupling factor (k_p) and mechanical quality factor (Q_m) were measured by a method similar to that of the IRE standard. The resonance and anti-resonance frequencies were obtained by using the maximum and the minimum of spectra admittance.

III. RESULTS AND DISCUSSION

A. *X-ray Diffraction Profile*

Fig. 1 shows the XRD patterns of sintered (1-x) Pb ($Zr_{0.52}$ $Ti_{0.48}$) O_3 – x Sm Cr O_3 (where x = 0.005, 0.01, 0.015, 0.02 and 0.025) ceramics. The tetragonal, rhombohedral and tetragonal-rhombohedral phases are identified by analysis of peaks [002 (tetragonal), 200 (tetragonal), 200 (rhombohedral)] in 2θ range of 10º–80°.

The XRD patterns confirm that all the PZTSC powders are pure and monophasic in nature, and free from the pyrochlore phases. As evident from the XRD patterns, the structure is tetragonal at SC concentrations up to x = 0.015. The co-existence of rhombohedral and tetragonal phases at x values equal or greater than 0.02 suggests that this composition (x ≥ 0.02) corresponds to MPB.

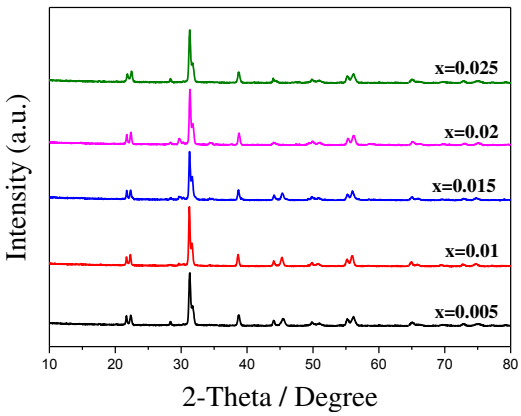

Fig. 1 XRD patterns of PZTSC ceramics with different SC contents in the 2θ range of 10º–80°, sintered at 1150 °C

B. *AFM Analysis*

Fig. 2 shows AFM images of ceramic samples of doped solid solutions: (1-x) Pb ($Zr_{0.52}$ $Ti_{0.48}$) O_3 – x Sm Cr O_3 with x=0.005, x=0.01, x=0.015, x=0.02 and x=0.025. Microstructural details, such as grain size and morphology as well as domain wall arrangements, can be observed from these micrographs. With the increase of SC content, the (1-x) Pb ($Zr_{0.52}$ $Ti_{0.48}$) O_3 – x Sm Cr O_3 ceramics become much denser, and their average grain size gradually decreases, as shown in Fig.2.

ISSN 2356-5608

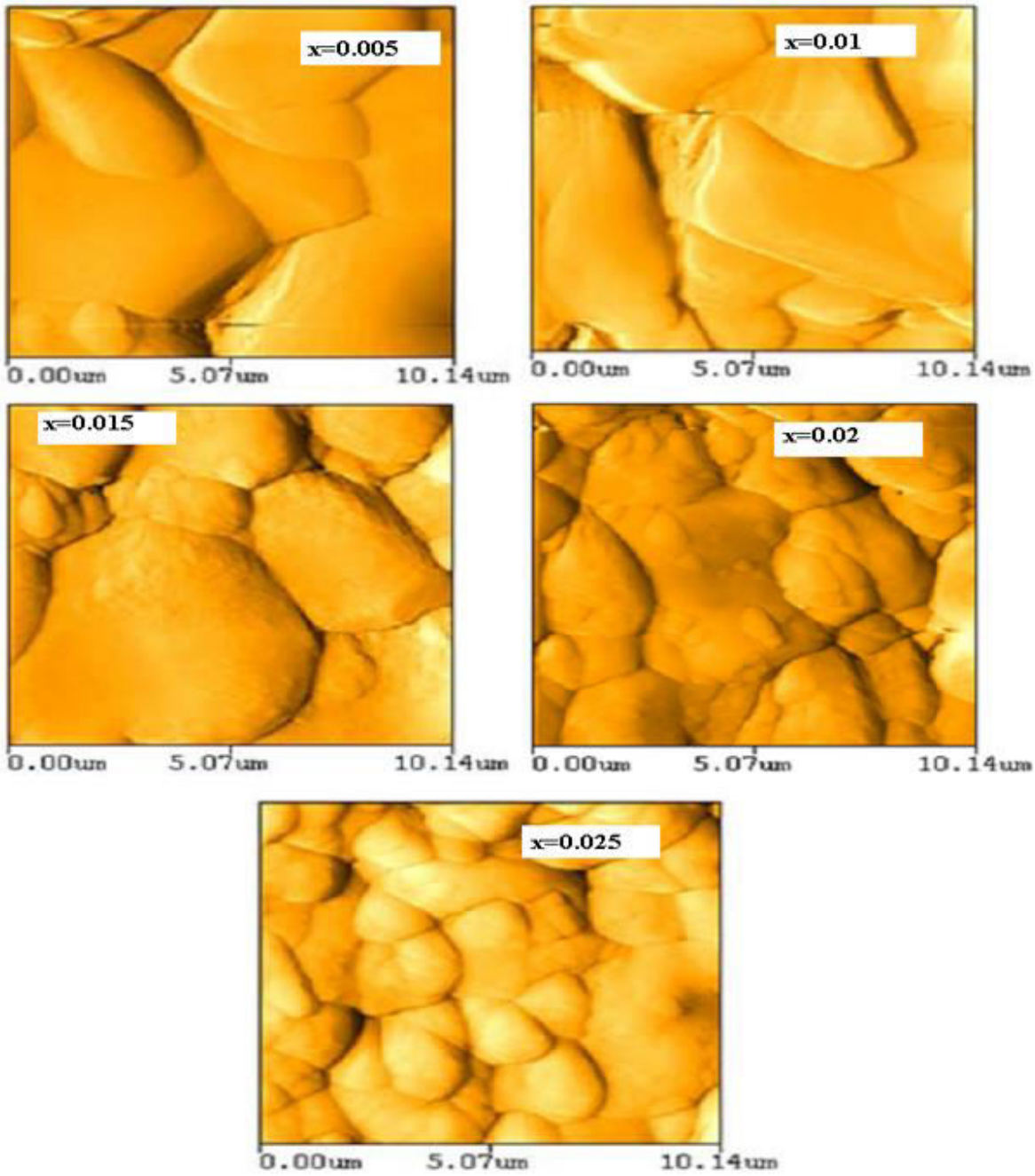

Fig. 2 AFM images of the (1-x) Pb ($Zr_{0.52}$ $Ti_{0.48}$) O_3 – x Sm Cr O_3 solid solutions with various compositions: x=0.005, x=0.01, x=0.015, x=0.02 and x=0.025

C. Density Measurement

Fig. 3 shows the relative density (i.e. the measured density divided by the theoretical density of PZT of 8.0 g/cm^3) of the ceramics as a function of the SC content. With increasing SC content, the density increases, reaching a maximum value of 7.91 g/cm^3 in samples with 0.025 wt.% Sm_2O_5 and Cr_2O_3.

In addition, the density results in Fig. 3 are consistent with the porosity variations shown in Fig. 2 which lead to the decreasing density. These results show that adding an appropriate amount of Sm_2O_5 and Cr_2O_3 can promote the densification behavior, because of the enhanced sintering activity. This may be due to mass transfer caused by oxygen vacancies via partial substitution of Cr^{3+} for Zr^{4+} and Ti^{4+}, which is used as a transferred carrier to accelerate mass mobility.

ISSN 2356-5608

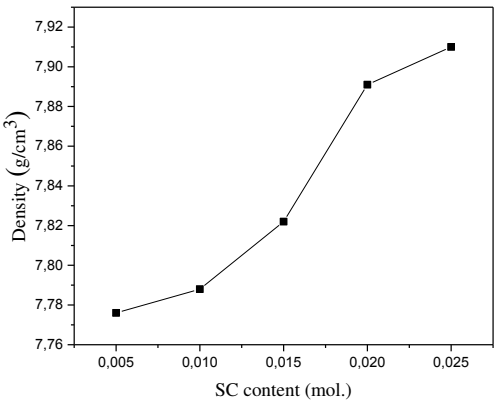

Fig. 3 Density of ceramics as a function of SC content

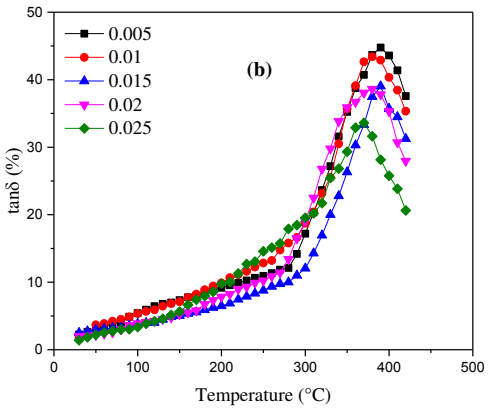

Fig. 4 Temperature dependence of (a) ε_r and (b) tanδ of the PZTSC ceramics with different SC contents

D. Dielectric Properties

The temperature dependence of the (a) dielectric constant (ε_r) and (b) losses (tanδ) for (1-x) Pb ($Zr_{0.52}$ $Ti_{0.48}$) O_3 – x Sm Cr O_3 ceramics with different SC contents at the frequency of 1kHz is presented in Fig. 4. It is observed that with the increase in Sm and Cr substitution, there is systematic decrease in phase transition temperature (Tc). The decrease in phase transition temperature is mainly due to dis-appearance of long range order co-operative phenomenon.

The dielectric constant increases with increase in Sm and Cr substitution and the losses (tanδ) are smaller for the denser samples (x=0.02 and 0.025).

The decrease in dielectric constant (ε_r) may be due to the dominance of 90° domains contribution to the dielectric properties after poling. Here in our case the aligned ~90° rotated domains after poling cause more mechanical stress and enhance the anisotropy that results in decrease in dielectric constant.

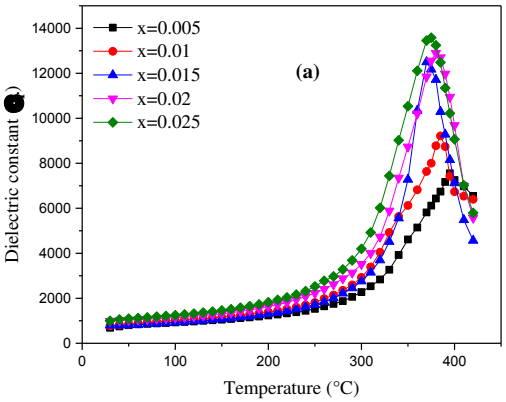

E. Piezoelectric Properties

Fig. 5 indicates the mechanical quality factor (Q_m), electromechanical coupling factor (K_p) and piezoelectric constant (d_{31}) as a function of SC content. As can be seen, K_p, d_{31} and Q_m show a similar variation with increasing SC content. K_p, d_{31} and Q_m both increase with increasing SC contents. K_p, d_{31} and Q_m reach their maximum (0.58, 293 pC/N and 745) at 0.025 (mol.) SC content.

The increase of Q_m may be due to the low-valence substitution of Cr^{3+} for Zr^{4+} and Ti^{4+}, which will lead to the appearance of oxygen vacancies to maintain electrovalence balance. The oxygen vacancies will produce a “pinning effect” on domain rotation; thereby, the material becomes “hard” [23, 24]. The increase of Q_m may be caused by the increasing density.

In addition, the changes of Q_m, K_p and d_{31} are complex and slightly different from traditional acceptor doping effects, because two factors act together to cause the variation of the electrical properties, i.e.,Cr^{3+} modification resulting in the development of hard piezoelectric behavior, and densification of the ceramics with Cr_2O_3 addition.

Therefore, under the combination of both of these effects, some electrical properties do not agree with the expected hard characteristics of this system.

ISSN 2356-5608

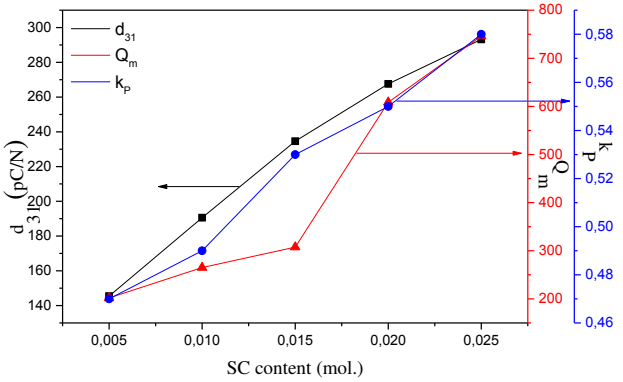

Fig. 5 Qm, Kp, and d_{31} of ceramics as a function of SC content

IV. Conclusions

Ceramic samples of (1-x) Pb $(Zr_{0.52}\ Ti_{0.48})\ O_3 - x$ Sm Cr O_3 (where x = 0.005, 0.01, 0.015, 0.02 and 0.025) were prepared by the conventional oxide-mixed method. The structure, microstructure, dielectric and piezoelectric properties were investigated systematically. XRD analysis reveals the co-existence of tetragonal and rhombohedral phases (MPB) were located near the SCX content of $x \geq 0.02$. The grain size in the modified microstructure decreases with the increase of Sm and Cr substitution. The SC addition promoted densification of ceramics and the highest density of 7.91 g/cm^3 was obtained at 0.025 wt.% SC addition. The room temperature dielectric constant (ε_r) and tangent loss (tanδ), piezoelectric coefficient d_{31}, electromechanical coupling factor k_p, and mechanical quality factor (Q_m) of 0.975 Pb $(Zr_{0.52}\ Ti_{0.48})\ O_3 - 0.025$ Sm Cr O_3 ceramics are 998, 1.405 %, 293 pC/N, 0,58, 745, respectively, which mean it has a great promise for ultrasonic motors.

References

[1] J. Xu, M. Yang, K. Gana , Y. Qu, X. Zhang, N. Ma, Y. Wanga, and J. Yang, "Enhanced piezoelectric properties of PZT ceramics prepared by direct coagulation casting via high valence counterions (DCC–HVCI)," *Ceramics International*, vol. 42, pp. 2821–2828, Nov. 2016.

[2] G. Tian , W. Deng , Y. Gao , D. Xiong , C. Yan , X. He , T. Yang , L. Jin , X. Chu , H. Zhang, W. Yan, and W. Yang, "Rich lamellar crystal baklava-structured PZT/PVDF piezoelectric sensor toward individual table tennis training," *Nano Energy*, vol. 59, pp. 574-581, Mar. 2019.

[3] Z. Zhang, J. Xu, L. Yang, S. Liu, J. Xiao, X. Li, X. Wang, and H. Luoa, "Design and comparison of PMN-PT single crystals and PZT ceramics based medical phased array ultrasonic transducer," *Sensors Actuators A*, vol. 283, pp. 273–281, Sep. 2018.

[4] J. Wu, Y. Mizuno, and K. Nakamura, "Ultrasonic motors with poly phenylene sulfide/alumina/PZT triple-layered vibrators," *Sensors Actuators A*, vol. 284, pp.158–167, Oct. 2018.

[5] S. Gholami, M. M. Mohebi, and B. Janipour, "Template-free formation of $Pb(Zr_{0.52}Ti_{0.48})O_3$ (PZT) nanorods," *J. Mater. Sci: Mater. Electron*, vol. 26, pp. 10087–10094, Sep. 2015.

[6] S. Hajra, P. Sharma, S. Sahoo, P. K. Rout, and R. N. P. Choudhary, "Processing and electrical properties of gallium-substituted lead zirconate titanate ceramics," *Applied Physics A*, vol. 123, pp. 786 –795, 2017.

[7] C. Cheng, D. YiZheng, G. Peng, S. Hu, H. Zhang, and J. Zhang, "The effects of Sm_2O_3 doping on properties of PNN–PZT ceramics near morphotropic phase boundary," *J. Mater. Sci: Mater. Electron*, vol. 28, pp. 1624–1630, Sep. 2017.

[8] C. P. Fernández, F. L. Zabotto, D. Garcia, and R. H. G. A. Kiminami, "In situ sol-gel co-synthesis at as low hydrolysis rate and microwave sintering of PZT/Fe_2CoO_4 magnetoelectric composite ceramics," *Ceramics* International, vol. 43, pp. 5925–5933, Jan. 2017.

[9] A. G. Znamenskii, A. M. Ionov, and V. A. Marchenko, "Gas Release in the Process of Thermal Treatment of Sputtered $Pb(Ti_{0.48}Zr_{0.52})O3$ Films," *Physics Solid State*, vol. 58, pp. 1239–1246, Jan. 2016.

[10] P. Zhou, K. Liang, Y. Liu, Z. Zheng, and T. Zhang, "Efect of interface coupling on magnetoelectric response of $Pb(Zr_{0.52}Ti_{0.48})O_3/La_{0.67}Sr_{0.33}MnO_3$ thin film under different strain states," *Applied Physics A*, vol. 124, pp. 670–675, 2018.

[11] J. R. Gatabi, S. Rahman, A. Amaro, T. Nash, J. Rojas-Ramirez, R. K. Pandey, and R. Droopad, "Tuning electrical properties of PZT film deposited by Pulsed Laser Deposition," *Ceramics International*, vol. 43, pp. 6008–6012, Jan. 2017.

[12] X. Chao, J. Wang, J. Pu, S. Zhang, and Z. Yang, " Aging behavior and electrical properties of low-temperature sintered (Ba, Ca)(Ti, Zr)O_3-Ba(Cu, W)O_3 ceramics and plate loudspeaker," *Sensors Actuators A*, vol. 237, pp. 9–19, Jan. 2016.

[13] Z. Xiao, X. Li, X. Dong, J. Tang, C. Wang, T. Zhang, S. Li, and L. B. Kong, "Sintering and electrical properties of commercial PZT powders modified through mechanochemical activation," *J. Mater. Sci.*, vol. 53, pp.13769–13778, Apr 2018.

[14] D. Bochenek, P. Niemiec, M. Adamczyk, Z. Machnik, and G. Dercz, "Dielectric properties of the multicomponent PZT-type solid solution," *Eur. Phys. J. B*, vol. 88, pp. 279–283, Oct. 2015.

[15] O. Namsar, S. Pojprapai, A. Watcharapasorn, and S. Jiansirisomboon, "Polarization fatigue in ferroelectric $Pb(Zr_{0.52}\ Ti_{0.48})O_3$-$SrBi_2O_9$ ceramics," *Electron. Mater. Lett.*, vol. 11, pp. 881–889, Feb. 2015.

[16] J. Yi, M. Shen, S. Liu, and S. Jiang, "Effects of PbO-B_2O_3 glass doping on the sintering temperature and piezoelectric properties of $0.35Pb(Ni_{1/3}Nb_{2/3})O_3$-$0.65Pb(Zr_{0.41}Ti_{0.59})O_3$ Ceramics," *Journal Electronic Materials*, vol. 44, pp. 2846–2851, Sep. 2015.

[17] X. Zong, and Z. Yang, "Effects of Fe_2O_3 Additive on the structure and piezoelectric properties of PZT-PFW-PMN Ceramics," *Journal Electronic Materials*, vol. 44, pp.258–262, Jan. 2015.

[18] J. Zeng, K. Zhao, X. Shi, X. Ruan, L. Zheng, and G. Li, "Large strain induced by the alignment of defect dipoles in(Bi^{3+},Fe^{3+}) co-doped $Pb(Zr,Ti)O_3$ ceramics," *Scripta Materialia*, vol. 142, pp. 20–22, Aug. 2018.

[19] Y. Zhang, J. Roscow, M. Xie, and C. Bowen, "High piezoelectric sensitivity and hydrostatic figures of merit in unidirectional porous ferroelectric ceramics fabricated by freeze casting," *Journal European Ceramic Society*, vol. 38, pp. 4203–4211, Apr. 2018.

[20] T. A. Babu, K. V. Ramesh, V. R. Reddy, D. L. Sastry, "Structural and dielectric studies of excessive Bi^{3+} containing perovskite PZT and pyrochlore biphasic ceramics," *Materials Science Engineering B*, vol. 228, pp. 175–182, Jan. 2018.

[21] Y. Yan, Y. Feng, and Z. Li, "The effect of uniaxial pressure, temperature and electric field, on the internal bias field in the lead-based piezoelectric ceramics," *Materials Letters*, vol. 164, pp. 248–251, Jan. 2016.

[22] A. Limpichaipanit, S. Somwan, and A. Ngamjarurojana, "Dielectric properties of PFN–PZT composites: From relaxor to normal ferroelectric behavior," *Ceramics International*, vol. 44, pp. 14797–14802, May. 2018.

[23] O. M. Zhigalina, D. N. Khmelenin, Y. A. Valieva, V. Y. Kolosov, A. O. Bokuniaeva, G. B. Kuznetsov, K. A. Vorotilov, and A. S. Sigov, "Structural Features of PLZT Films," *Crystallography Reports*, vol. 63, pp .646–655, 2018.

[24] K. Guo, Q. Mou, T. He, H. Kong, and R. Zhang, "Ferroelectric, ferromagnetic, magnetodielectric and in-plane ME coupling properties of $Pb(Zr_{0.52}Ti_{0.48})O_3$–$Bi_{0.9}Nd_{0.1}FeO_3$ bilayer nano-films prepared via Sol–gel processing," *J. Mater. Sci: Mater. Electron.*, vol. 28,1 pp. 971–1975, Jan. 2017.

ISSN 2356-5608